

## Transformation of Organic Cacao (*Theobroma cacao*) Husk into Commercial

## Transformación de cáscara de Cacao Orgánico (*Theobroma cacao*) en productos comerciales

Luis Fernando Valencia<sup>1</sup>  Ana María Tovar<sup>1</sup>  Aída Luz Villa<sup>1</sup>  

<sup>1</sup>Environmental Catalysis Research Group, Chemical Engineering Department, Engineering Faculty, Universidad de Antioquia UdeA. Medellín, Colombia.

### Abstract

**Introduction:** agroindustrial wastes can be transformed to mitigate the negative impacts associated with their disposal. In cocoa production, cocoa pod husk (CPH) constitutes between 67% and 76% of the total cocoa weight. This study focuses on the potential of CPH as a valuable resource for producing activated carbon, cellulose, and potassium hydroxide (KOH).

**Objective:** The objective of this research was to characterize and transform the CPH obtained from an organic crop in San Bernardo-Ibagué (Colombia) into activated carbon, cellulose, and KOH.

**Methods:** activated carbon was produced through chemical activation using KOH, with a specific procedure for characterizing the obtained product through thermal analysis (TGA) and nitrogen adsorption and desorption isotherms. For cellulose extraction, an alkaline treatment with 2% w/w NaOH was followed by a bleaching process with 2.5% w/w sodium hypochlorite. KOH was obtained by first extracting potassium carbonate and then causticizing it.

**Results:** activated carbon (AC) was produced with a yield of 25.6%, exhibiting a surface area of 468 m<sup>2</sup>/g, a mean pore diameter of 10.8 nm, and a total pore volume of 0.228 cm<sup>3</sup>/g, with 60% fixed carbon, 27% volatile material, 6% ash, and 6% moisture.

**Conclusions:** the transformation of cocoa pod husk into activated carbon, cellulose, and KOH provides a sustainable approach to managing agroindustrial waste, generating valuable products with significant potential for various applications. The results obtained demonstrate the feasibility of utilizing CPH as a resource in agroindustrial processes.

**Keywords:** : cocoa pod husk, Activated carbon, Cellulose, Potassium hydroxide, Agroindustrial wastes

### How to cite?

Valencia, L.F., Tovar, A.M., Villa, A.L. Transformation of Organic Cacao (*Theobroma cacao*) Husk into Commercial Products Ingeniería y Competitividad, 2024, 26(3)e-20713519

<https://doi.org/10.25100/iyc.v26i3.13519>

Recibido: 31-01-24  
Evaluado: 06-05-24  
Aceptado: 22-07-24  
Online: 24-09-24

### Correspondence

aida.villa@udea.edu.co  
Carrera 80 N.º65-223. Medellín  
Colombia.



## Resumen

**Introducción:** los desechos agroindustriales pueden ser transformados para mitigar los impactos negativos asociados con su disposición. En la producción de cacao, la cáscara de la mazorca de cacao (CMC) constituye entre el 67% y el 76% del peso total del cacao. Este estudio se centra en el potencial de la CMC como un recurso valioso para la producción de carbón activado, celulosa y hidróxido de potasio (KOH)..

**Objetivo:** caracterizar y transformar la CMC obtenida de un cultivo orgánico en San Bernardo-Ibagué (Colombia) en carbón activado, celulosa y KOH.

**Métodos:** se produjo carbón activado mediante activación química con KOH, utilizando un procedimiento específico para caracterizar el producto obtenido a través de análisis térmico (TGA) y la isoterma de adsorción y desorción de nitrógeno. Para la extracción de celulosa, se realizó un tratamiento alcalino con NaOH al 2% p/p, seguido de un proceso de blanqueo con hipoclorito de sodio al 2.5% p/p. El KOH se obtuvo extrayendo primero el carbonato de potasio y luego causticizándolo.

**Resultados:** el carbón activado (CA) se produjo con un rendimiento del 25.6% y presentó una superficie de 468 m<sup>2</sup>/g, un diámetro medio de poro de 10.8 nm, y un volumen total de poro de 0.228 cm<sup>3</sup>/g, con un 60% de carbono fijo, 27% de material volátil, 6% de ceniza y 6% de humedad.

**Conclusiones:** la transformación de la cáscara de la mazorca de cacao en carbón activado, celulosa y KOH ofrece un enfoque sostenible para la gestión de desechos agroindustriales, generando productos valiosos con un alto potencial para diversas aplicaciones. Los resultados obtenidos demuestran la viabilidad de utilizar la CMC como recurso en procesos agroindustriales.

**Palabras clave:** cáscara de mazorca de cacao, Carbón activado, Celulosa, Hidróxido de potasio, Desechos agroindustriales

### Why was it conducted?:

Cocoa production in Colombia is one of the most important agro-industrial activity, generating large amounts of cocoa pod husk that must be disposed in an adequate way for avoiding pollution. Furthermore, high value-added products can be obtained from cocoa pod husk in a circular economy approach.

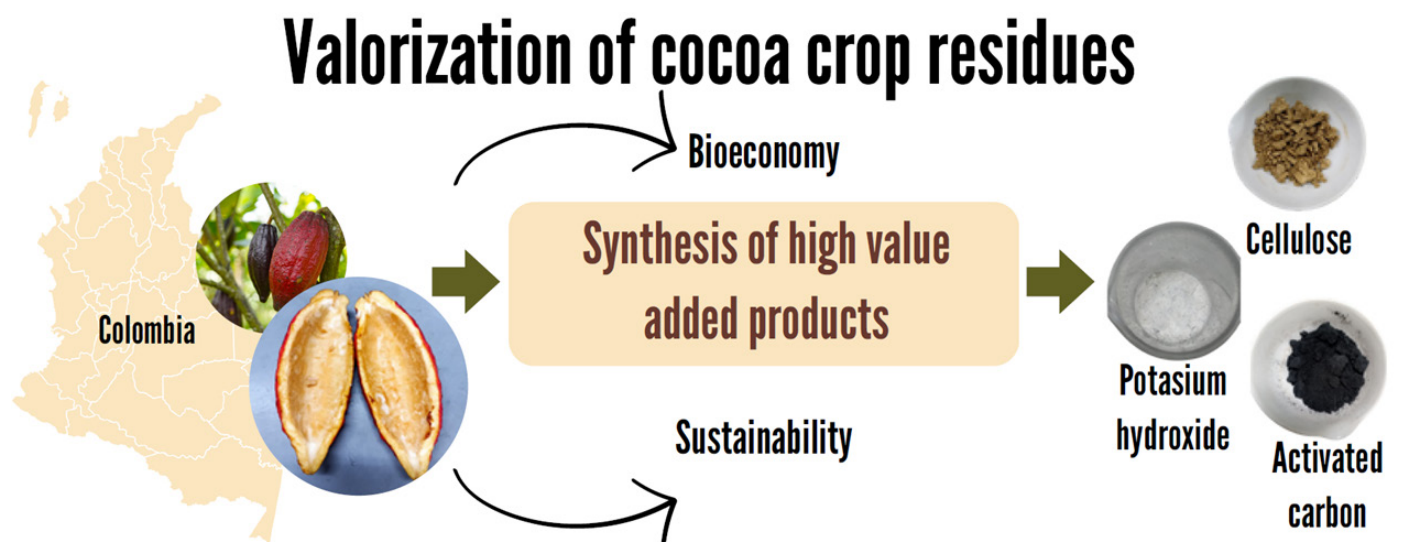
### What were the most relevant results?

Cocoa pod husk was transformed into a mesoporous activated carbon with a surface area of 468 m<sup>2</sup>/g, the solid was used as support of Zn and the obtained catalyst was active for terpene oxidation. Cellulose extraction process with a 32.2 % yield and 84.5 % purity of  $\beta$ -cellulose was reached.

### What do these results contribute?

The research shows several ways of given value to a agroindustrial waste as Cocoa pod husk. As a source of material for bio-medical application, biopolymer production, and catalyst synthesis.

## Graphical Abstract



## Introduction

The disposal of large quantities of organic wastes is a problem because the generated pollution (1); therefore, the conversion of biomass into bioproducts and bioenergy is an innovative aspect of pursuing the principles of the circular economy, the purpose of which is to increase renewable sources and reduce the consumption of raw materials and energy (2). The agro-industrial wastes are mainly composed of cellulose, hemicellulose, and lignin (lignocellulosic fibers) (3), due to their composition, agro-industrial wastes have a potential for multivalORIZATION. They can be used to produce a wide range of valuable products, such as biofuels, biopolymers, biofertilizers, enzymes, nutraceuticals and biogas, among others (4). Cocoa (*Theobroma cacao*) production in Colombia is one of the most important agro-industrial activity due to its direct impact in the social and economic development of smallholder farmers, many of them located in vulnerable and post-conflict regions (5). The cocoa pod husk (CPH) is derived from the cocoa processing and for each kilogram of cocoa produced, it is generated 10 times more CPH (6). For the CPH residues management some practices of minimum value-added are implemented; the most common methods to manage CPH are leaving the residues on the countryside with no treatment or breaking the CPH to accelerate its decomposition turning it into a compost product for the soil improvement (7). The development of strategies for the valorization of CPH into commercially valuable products has gained great importance due to the potential of its chemical composition. CPH has been used for soap and activated carbon (AC) manufacturing and its transformation through biotechnological processes for biofuel production (8). CPH has been used for obtaining pectin, dietary fibers, polyphenols, methylxanthines, and phytosterols (9); also, for the production of organic fertilizers through composting, for animal feed, and bioenergy production (10).

Cellulose is a non-toxic material, it is stable, biodegradable, and accessible, making it highly useful for a wide range of applications (11). The diversity and abundance of cellulose and nanocellulose materials from agro-industrial waste, compared to other materials, have opened the door to a wide

range of applications and the development of new products, particularly in the food industry. Other product that can be obtained from agro-industrial wastes is AC, that can be obtained by physical or by chemical activation, which offers advantages of reduced activation period, higher surface area and pore volume compared to physical activation (12). The low price and high availability of CPH compared to traditional activated carbon precursors, such as anthracite, coal, or peat, could increase its economic potential by reducing overall production costs (13). Furthermore, CPH is used as precursor in the preparation of potassium salts (14); the ash produced when CPH are burned is rich in potash (15). It was reported that extracted potash from cocoa pod husk was applied as an alkalinizing agent in the processing of dutch cocoa (16). The design and optimization of an automated reactor for an annual KOH production of 35,000 tons from the cocoa pod husk was also reported (17).

The carbon footprint associated with the inadequate disposal of agro-industrial waste generates an annual accumulation equivalent to 3.3 billion tons of CO<sub>2</sub> in the atmosphere (4); therefore, the development of high value-added products from agro-industrial waste, as CPH, is an alternative to reduce negative environmental impacts. This report presents the transformation of CPH into commercially valuable products such as cellulose, potassium hydroxide, and activated carbon; furthermore, the obtained activated carbon was used as support in the synthesis of a catalyst that was used in the transformation of some terpenes after impregnation with zinc, which has not previously reported; furthermore, the alkaline treatment for cellulose extraction was carried out with a low NaOH concentration.

## Materials and methods

### Pretreatment and analysis of cocoa pod husks

The CPH was obtained from a mixture of Criollo and Trinitario cocoa varieties cultivated in organic farms of the association "Héroes del Cultivo" in the rural zone of San Bernardo-Ibagué (Colombia), located at an altitude of 1285 meters above sea level with an average temperature of 28 °C. The CPH was washed with distilled water to remove impurities, then it was cut into pieces and dried in an oven at 105 °C for 14 h. Finally, the dried material was ground to a particle size < 1 mm using an Amber coffee grinder. Proximate analysis of the CPH was performed using standardized methodologies, including % moisture content (ISO 18134-3:2015), % volatile matter (ISO 18123:2015), % ash content (ISO 18122:2015), % hemicellulose (Van Soest method, AOAC 2002.49), % cellulose (Van Soest method, AOAC 973.18), % lignin (Van Soest method using sulfuric acid), and potassium content (SM 3111B); the % fixed carbon was evaluated using Eq. (1).

$$\%Fixed\ carbon = 100 - \%Volatile\ matter - \%Ashes - \%Moisture \quad (1)$$

The morphology of the sample was observed using scanning electron microscopy (SEM) with vacuum emission, using a Denton Vacuum Desk IV equipment and a JSM-6490IIv microscope. The sample was coated with a thin layer of gold, mounted on a graphite tape for analysis, and images were taken with an acceleration voltage of 11.3 kV. Elemental analysis was performed using X-ray microprobe - EDX (INCA PentaFETx3 Oxford Instruments).

### Activated carbon production from cocoa pod husks

The dried and triturated sample with a particle size of < 1 mm was impregnated with potassium hydroxide (KOH, Merck; assay ≥ 85%) using a mass ratio of 0.5:1 (KOH: sample) in a 250 mL beaker. Distilled water was added to the mixture with a mass ratio of 3:1 (water: mixture). The impregnation was carried out for 1 h at 23 °C and 500 rpm; the impregnated sample was left at room temperature for 12 h, and then dried in a convection oven at 80 °C for 6 h. The dried sample was pyrolyzed at 500 °C for 3 h with a heating rate of 10 °C/min under a nitrogen flow of 100 cm<sup>3</sup>/min. After the pyrolysis, the activated carbon was washed with 32 mL of 1 M hydrochloric acid (HCl) and 35 mL of distilled water to remove residual potassium ions and to adjust the pH to ~7. The sample was dried at 80 °C for 3 h in a convective oven (18). The yield of AC was calculated with Eq. (2), as the ratio between the obtained AC and the dried CPH used as raw material. The textural properties of the activated carbon were determined using a Micromeritics chemisorption analyzer Model ASAP 2020 PLUS. Initially the sample was degasified at 350 °C for 3 h under vacuum, followed by the nitrogen

adsorption and desorption at  $-196\text{ }^{\circ}\text{C}$ , and the data were obtained in a relative pressure ( $P/P_0$ ) range of 0.1 to 0.998. The pore diameter was determined by the BJH (Barrett, Joyner, and Halenda) method and the surface area was calculated with the t-plot method. In a thermogravimetric analyzer TGA Q500, 8.825 mg of sample with a particle size of  $90\text{ }\mu\text{m}$  were treated with a nitrogen flow rate of  $1\text{ cm}^3/\text{min}$ ; the sample was heated at  $10\text{ }^{\circ}\text{C}/\text{min}$  from room temperature to  $107\text{ }^{\circ}\text{C}$  and held at this temperature for 5 minutes. Then the sample was heated at  $20\text{ }^{\circ}\text{C}/\text{min}$  to  $900\text{ }^{\circ}\text{C}$  and maintained at this temperature for 7 minutes. Finally, the sample was cooled to  $650\text{ }^{\circ}\text{C}$  and switched to an oxygen flow rate of  $1\text{ cm}^3/\text{min}$ , with an increase of temperature at  $2\text{ }^{\circ}\text{C}/\text{min}$  to  $750\text{ }^{\circ}\text{C}$  and maintained at this temperature for 2 h.

$$\frac{\text{Obtained solid (g)}}{\text{Dried CPH (g)}} * 100 \quad (2)$$

### Synthesis of Zn catalyst with CPH activated carbon

The synthesis of heterogeneous zinc catalyst supported on activated carbon obtained from CPH was performed by incipient impregnation. The amount of zinc nitrate hexahydrate (Merck, 99 %) for obtaining a nominal concentration of 1 % of the metal on the solid, was diluted in 10 mL of distilled water; the solution was mixed with activated carbon for 20 min at 500 rpm and room temperature. Then, the obtained solid was dried at  $80\text{ }^{\circ}\text{C}$  for 3 h and pyrolyzed with a nitrogen flow of  $100\text{ ml min}^{-1}$  at  $500\text{ }^{\circ}\text{C}$  for 1 h at  $10\text{ }^{\circ}\text{C min}^{-1}$ . The obtained solid was named as ZnAC.

### Epoxidation of $\alpha$ -pinene, limonene and $\beta$ -pinene

The epoxidation of R-(+)- $\alpha$ -pinene, S-(-)- $\beta$ -pinene, and R-(+)-limonene of Sigma Aldrich brand was carried out in 2 mL vials covered with inert silicon septa immersed in a Radley tech hot plate with magnetic stirring using the Payne system. In a typical experiment ( $50\text{ }^{\circ}\text{C}$ , 750 rpm, and 2 h), a substrate: hydrogen peroxide : acetonitrile : acetone : water : catalyst mass ratio of 1: 0.86: 15.35: 19.17: 29.41: 1.66 was used. At the end of the reaction, manganese (II) oxide was added to decompose the excess hydrogen peroxide. The products were identified by gas chromatography using an Agilent 7890A gas chromatograph with FID and Agilent 5975C mass detector, using He as carrier gas; a silica HP-5MS capillary column (30 m, 0.25 mm, and  $0.25\text{ }\mu\text{m}$ ) and flame ionization detector (FID) were used. The velocity and flow rate of the carrier gas was  $30.5\text{ cm/s}$  and  $2.2\text{ mL/min}$ , respectively. The oven temperature was  $70\text{ }^{\circ}\text{C}$  for 1 min and then increased to  $90\text{ }^{\circ}\text{C}$  ( $10\text{ }^{\circ}\text{C}/\text{min}$ ) for 0.5 min, then raised to  $110\text{ }^{\circ}\text{C}$  ( $10\text{ }^{\circ}\text{C}/\text{min}$ ) for 0.5 min, then to  $130\text{ }^{\circ}\text{C}$  ( $10\text{ }^{\circ}\text{C}/\text{min}$ ) for 0.5 min and finally up to  $160\text{ }^{\circ}\text{C}$  ( $15\text{ }^{\circ}\text{C min}^{-1}$ ) for 1 min. The injection volume was  $1\text{ }\mu\text{L}$  in split mode (25:1) with injector temperature of  $250\text{ }^{\circ}\text{C}$ . Compound identification was performed using the NIST database<sup>5</sup>. Conversion and selectivity were determined using Eq. (3) and Eq. (4), respectively.

$$\% \text{ Conversion} = \frac{\sum A_{\text{products}}}{\sum A_{\text{products}} + A_{f,t}} * 100 \quad (3)$$

$$\% \text{ Selectividad} = \frac{(A_f)_{\text{product}}}{\sum A_{\text{products}}} * 100 \quad (4)$$

Where is the area of the products,  $(A_f)_{\text{product}}$  is the final area of each product and  $A_{f,t}$  is the final area of the terpene ( $\alpha$ -pinene, limonene or  $\beta$ -pinene).

### Cellulose extraction from cocoa pod husks

The extraction of cellulose included alkaline treatment and bleaching process. In the alkaline treatment, dried and triturated CPH was treated with a 2% w/w aqueous solution of sodium hydroxide at a CPH to sodium hydroxide solution ratio of 1:20 (w/v) for 2 h at  $90\text{ }^{\circ}\text{C}$ ; then, the solid was vacuum filtered to separate the solid material, washed five times with 40 mL of distilled water to completely remove the alkali, and dried at  $80\text{ }^{\circ}\text{C}$  for 5 h in a convective oven (19). The yield of cellulose extraction was calculated with Eq. (2), as the ratio between the obtained cellulose and the dried CPH used as raw material. After the alkaline treatment, the fibers were treated with a 2.5% w/w aqueous solution of sodium hypochlorite at a solid to liquid ratio of 1:20 (w/v) for 1.5 h at  $80\text{ }^{\circ}\text{C}$ . The mixture was then cooled and filtered with distilled water until reaching a neutral pH; the bleached fibers were dried at  $80\text{ }^{\circ}\text{C}$  for 3.5 h in a convective oven and weighed (20).



The  $\alpha$ -cellulose content of the extracted cellulose was determined following the TAPPI 203m 58 norm. The extracted cellulose was characterized by several techniques. The Fourier Transform Infrared (FTIR) analysis was carried out in a Perkin Elmer Spectrum 65 FTIR Spectrometer, through transmittance in the range of 4000-400  $\text{cm}^{-1}$ , with 20 scans and a resolution of 4  $\text{cm}^{-1}$ . In a thermogravimetric analyzer TGA Q500, 5.07 mg of sample with a particle size of 90  $\mu\text{m}$  were treated with a nitrogen flow rate of 60  $\text{cm}^3/\text{min}$ ; the sample was heated at 10  $^\circ\text{C}/\text{min}$  from room temperature to 800  $^\circ\text{C}$  and held at this temperature for 5 minutes. XRD analysis was performed on a Malvern-PANalytical Model Empyeon 2012, with Pixel 3D detector and Cu source ( $\lambda = 1.541874 \text{ \AA}$ ) at 45kV and 40 mA; in the range of 10 - 50 $^\circ$  ( $2\theta$ ) with a scanning step of 0.05 $^\circ$ ; the crystallinity index (21) was calculated using the Eq (5).

$$\% \text{Crystallinity index} = \left(1 - \frac{I_{am}}{I_m}\right) * 100 \quad (5)$$

where,  $I_{am}$  is the intensity in the amorphous region (17–19 $^\circ$ ) and  $I_m$  is the maximum intensity at  $2\theta = 22.3^\circ$ .

The apparent size of the crystal was calculated with the Debye-Scherrer equation, Eq (6).

$$L = \frac{k*\lambda}{\beta*\cos(\theta)} \quad (6)$$

where, L is the crystal apparent size (nm),  $\lambda$  is the wavelength of applied radiation (nm),  $\theta$  is the diffraction angle (radians) where the more intense peak is obtained, k is the Scherrer's constant that is 0.9 and  $\beta$  is half-width of the selected peak (radians).

#### KOH extraction from cocoa pod husks

The KOH extraction involved potassium carbonate extraction and causticization of potassium carbonate to potassium hydroxide. For the potassium carbonate extraction process, the dried and ground material was initially calcined at 650  $^\circ\text{C}$  with an airflow for 1 h at a heating rate of 7  $^\circ\text{C}/\text{min}$ ; then, the ashes were mixed with distilled water at a mass ratio of 1:10 at 80  $^\circ\text{C}$  and 500 rpm for 1 h. The obtained suspension was vacuum-filtered, and the liquid from the filtration was evaporated at 90  $^\circ\text{C}$  (19), then, in the causticization of potassium carbonate ( $\text{K}_2\text{CO}_3$ ), 0.4593 g of calcium hydroxide was added with 25 mL of deionized water. The mixture was slowly heated to 80  $^\circ\text{C}$  for the precipitation of calcium carbonate, which was separated from the soluble KOH by vacuum filtration. The filtrate (aqueous KOH) was evaporated to obtain crystals followed by recrystallization to obtain pure KOH crystals (22).

The morphology of the sample was observed using SEM. The quantification of  $\text{K}_2\text{CO}_3$  and KOH concentrations was performed using a reported method (23) with some modifications. A mass of 0.6 g of the obtained solids was weighed in a 250 mL beaker and mixed with 40 mL of distilled water at 300 rpm until a homogeneous mixture was achieved. Then, two drops of phenolphthalein indicator were added, and the mixture was titrated with 0.1 M HCl solution until a colorless mixture was obtained. After completing this process, two drops of methyl orange indicator were added, and the mixture was titrated with 0.1 M HCl solution until a pink color appeared in the mixture.

## Results and discussion

### Cocoa pod husks characterization

The CPH was characterized on a dry basis using proximate analysis (ash, fixed carbon, volatile matter including cellulose, hemicellulose, and lignin) and the results are shown in Table 1. The characteristics of the analyzed CPH are similar to reported values (5, 7, 18, 24) for moisture (3.2 - 10.9%), ash (2.2 - 8.8%), fixed carbon (19.3 - 21.4%), and volatile matter (59.4 - 75.3%).

Table 1. Proximal analysis of the CPH on dry basis

	This work	(5)	(7)	(18)	(24)
Moisture (%)	3.57	3.2	n.r.	10.91	10.5
Volatile matter (%)	72.9	75.3	n.r.	61.17	59.4
Ash (%)	8.48	2.2	n.r.	8.14	8.8
Fixed carbon (%)	15.0	19.3	n.r.	19.78	21.4
Hemicellulose (%)	52.1	n.r.	8.7 - 12.8	n.r.	21.2
Celullose (%)	23.7	n.r.	19.7 - 26.1	n.r.	23.2
Lignin (%)	16.5	n.r.	14 - 28	n.r.	15
K (%)	2.80	n.r.	2.8 - 3.8	n.r.	n.r.

n.r.: not reported.

Fig. 1 presents the corresponding DTG and TGA profiles of the CPH; the thermochemical decomposition of the vegetal material (volatile matter) can be represented by three main kinetics corresponding to the degradation of hemicellulose, cellulose, and lignin (25). When comparing the results of this study with the reported analysis (6) regarding the content of cellulose (19.7 - 26.1%), hemicellulose (8.7 - 12.8%), lignin (14 - 28%), and potassium (2.8 - 3.8%), it can be concluded that they are similar to the values obtained in this study for cellulose (23.7%), lignin (16.5%), and potassium (2.8%). The observed differences can be related to factors such as soil fertility used for cultivation, rainfall pattern during the plant's life (and other climatic factors), as well as anthropogenic reasons (26).

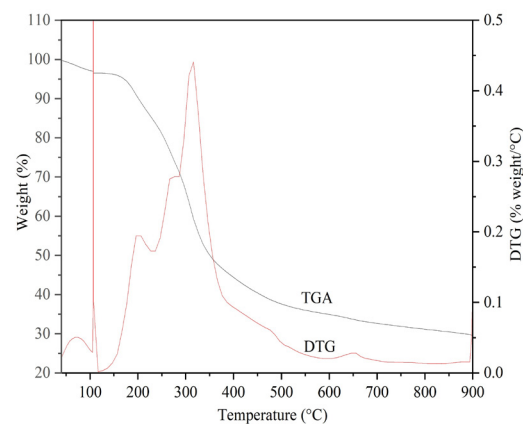


Figure 1. TGA/DTG curves of the cocoa pod husks on dry basis

### Characterization of the activated carbon obtained from cocoa pod husks

The textural characteristics such as specific surface area, average pore diameter, and total pore volume of the activated carbon obtained from the activation of CPH with KOH (CACKOH) are presented in Table 2; Fig. 2 shows the  $N_2$  adsorption-desorption isotherm at 77 K of CACKOH. The CACKOH has a specific surface area of 467.5  $m^2/g$ , with an average pore diameter of 10.8 nm and a total pore volume of 0.228  $cm^3/g$ . Results from the literature are also provided for comparison purposes of different lignocellulosic residues for the synthesis of activated carbon, using the same activating agent and pyrolysis temperature but with different pyrolysis time, the obtained activated carbons show a significant difference in pore diameter.

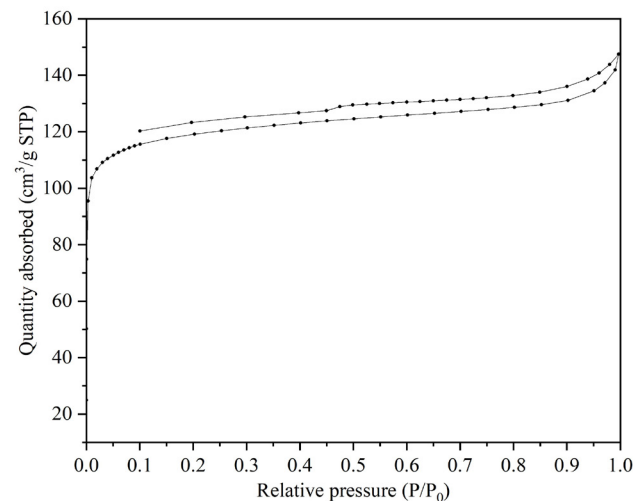


Figure 2. Nitrogen adsorption-desorption isotherm of CACKOH

Table 2 Textural properties of activated carbon obtained from several biomasses using KOH as activating agent

Biomasa	$R_i$ (w/w)	$T_p$ (°C)	$t_p$ (h)	$S_{BET}$ (m <sup>2</sup> /g)	$V_T$ (cm <sup>3</sup> /g)	$D_p$ (nm)	Reference
CPH	0.5:1	500	3.0	467.5	0.228	10.8	This work
CPH	0.5:1	500	0.5	483	0.266	2.21	(18)
CPH	0.5:1	500	n.r.	348.8	0.184	2.19	(27)
Poplar sawdust	1:1	500	n.r.	385.9	0.167	n.r.	(28)
Tobacco stem	0.5:1	600	1.5	500.8	0.304	n.r.	(29)
Rice husk	2:1	750	1.0	682.6	0.401	7.21	(30)
Arhar stalks	2:1	800	2.0	304.7	0.177	n.r.	(31)

$R_i$ : mass ratio of KOH: biomass,  $S_{BET}$ : specific BET surface area,  $V_T$ : total pore volume,  $D_p$ : pore diameter,  $t_p$ : pyrolysis time. n.r.: not reported.

The CACKOH was characterized on a dry basis through proximate analysis (ash, fixed carbon, volatile matter, cellulose, hemicellulose, and lignin). It has been reported that from room temperature to 150 °C corresponds to moisture loss, between 150-250 °C to hemicellulose decomposition, between 250-380 °C corresponds to cellulose decomposition (26); lignin decomposes in a range of 250-800 °C (32). Fig. 3 shows the temperatures ranges in TGA analysis for the degradation of compounds present in CACKOH. There are four weight loss stages under N<sub>2</sub> atmosphere: from 20 °C to 140 °C (6.36 %), from 140 °C to 210 °C (0.66 %), from 210 °C to 320 °C (1.11 %), from 310 °C to 480 °C (3.41 %); furthermore, from 480 °C to 900 °C with cooling to 650 °C, the weight loss is 21.77 %. Subsequently, when the atmosphere was switched to O<sub>2</sub> in the temperature range of 650-750 °C for 15 minutes, the material was completely carbonized to quantify the ash content. The volatile matter and the fixed carbon contents obtained in this study are like the values found in the activated carbon from yerba mate (33).



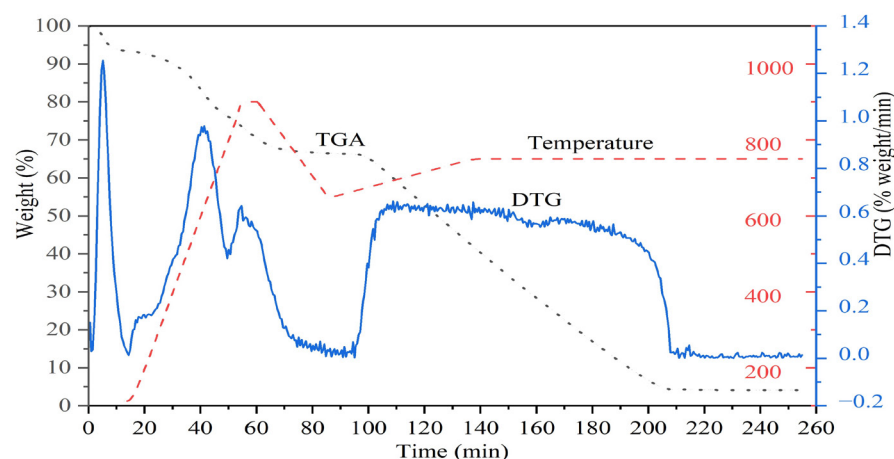


Figure 3. TGA/DTG curves of activated carbon from cocoa pod husks

The morphology of CPH and activated carbon is shown in Fig. 4a and Fig. 4b, respectively. The morphology of CPH shows a grooved surface while CACKOH shows irregular morphology with pore formation. This phenomenon is attributed to the effectiveness of KOH activation, due to the ability of K to form intercalation compounds with carbon; additionally, the  $K_2O$  formed during the KOH activation process is reduced to K by carbon, resulting in carbon gasification with subsequent  $CO_2$  emission leading to pore formation (34).

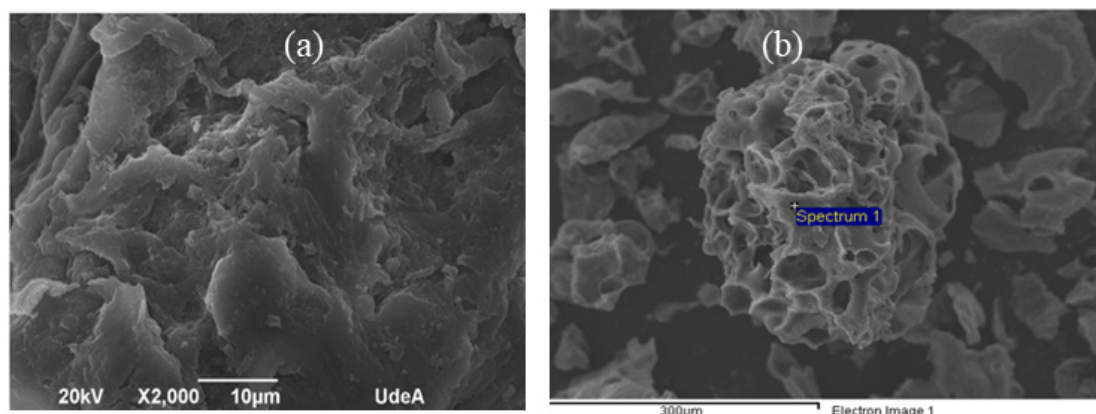


Figure 4. SEM images of cocoa pod husk (a) and obtained activated carbon (b)

#### Oxidation of $\alpha$ -pinene, $\beta$ -pinene and limonene

The oxidation of  $\alpha$ -pinene,  $\beta$ -pinene and limonene was performed using the Payne system where  $H_2O_2$  reacts with acetonitrile to form peroxyacetamide acid which acts as an oxygen atom donor to the double bond of the terpenes, forming acetamide as a by-product. Although acetonitrile can act as a solvent, improvements in the activity of the reaction have been described by adding external solvent and catalyst activators. For example, acetone and an excess of  $H_2O$  have shown to increase the activity for the epoxidation of styrene, using hydrotalcite as a catalyst. An optimum mass ratio of 1 : 3.2 : 15.35 : 19.17 : 29.41 : 1.2 (substrate :  $H_2O_2$  :  $CH_3CN$  : acetone :  $H_2O$  : catalyst) has been reported using MgO as catalyst (35). Fig. 5 shows terpene conversion and product selectivity over ZnAC catalyst; at 6 h,  $\alpha$ -pinene conversion was 97 % with a selectivity of 95 % towards  $\alpha$ -pinene epoxide,  $\beta$ -pinene conversion was 100 % and selectivity of 82 % towards  $\beta$ -pinene epoxide was obtained; the conversion of limonene was 64 % and the selectivity towards 1,2-limonene epoxide

was 87 %. In addition, no catalytic activity was evidenced in the oxidation of  $\alpha$ -pinene,  $\beta$ -pinene and limonene with the unimpregnated activated carbon zinc. Oxidation of  $\beta$ -pinene using the Pyne system with MgO has been reported with 100 % conversion and 74 % selectivity towards  $\beta$ -pinene epoxide (35). As low environmental impact, health risk and cost are desirable characteristics of a heterogeneous catalytic system, catalyst based on activated carbon from agro-industrial wastes are promising materials for terpene oxidation.

### Cellulose characterization

The extraction of cellulose from CPH was carried out through an alkali treatment and bleaching, resulting in a yield of 32.4% based on the initial dry mass of CPH and a concentration of 84.5% of  $\alpha$ -cellulose. Other authors have reported cellulose extraction from different agro-industrial wastes by alkaline treatment; pineapple crown waste with a content of 84.5 %  $\alpha$ -cellulose (36), royal palm waste with a yield of 63.1 % and 61.1 %  $\alpha$ -cellulose (37), mango seed with a yield of 22.8 % and 86.1 %  $\alpha$ -cellulose (38).

Fig. 6 shows the XRD pattern of cellulose extracted from CPH, in which the peaks at  $2\theta$  of around  $15.9^\circ$ ,  $22.3^\circ$  and  $34.6^\circ$  are characteristics of type I cellulose (39). The crystalline structure of cellulose I is a mixture of two different crystalline forms, cellulose  $I_\alpha$  (triclinic) and  $I_\beta$  (monoclinic). The crystallinity index was 79.34 % for the extracted cellulose; a high crystallinity provides higher strength, whereas low crystallinity enhances elongation, water intake, and chemical reaction sites (21). It has been reported that the crystallinity index of microcrystalline cellulose is between 60 and 80% (40) and that it is of around 70–90% for nanocrystalline cellulose (41). The crystallite size of the cellulose that was estimated by XRD using the Debye-Scherrer (Eq. 6) correlation was 23.6 nm, that corresponds to nanoparticles scale (42).  $\alpha$ -Cellulose has been identified as a promising material for biomedical applications because of its advantages over traditional biopolymers, owing to its high availability in natural resources and its low toxicity (43).

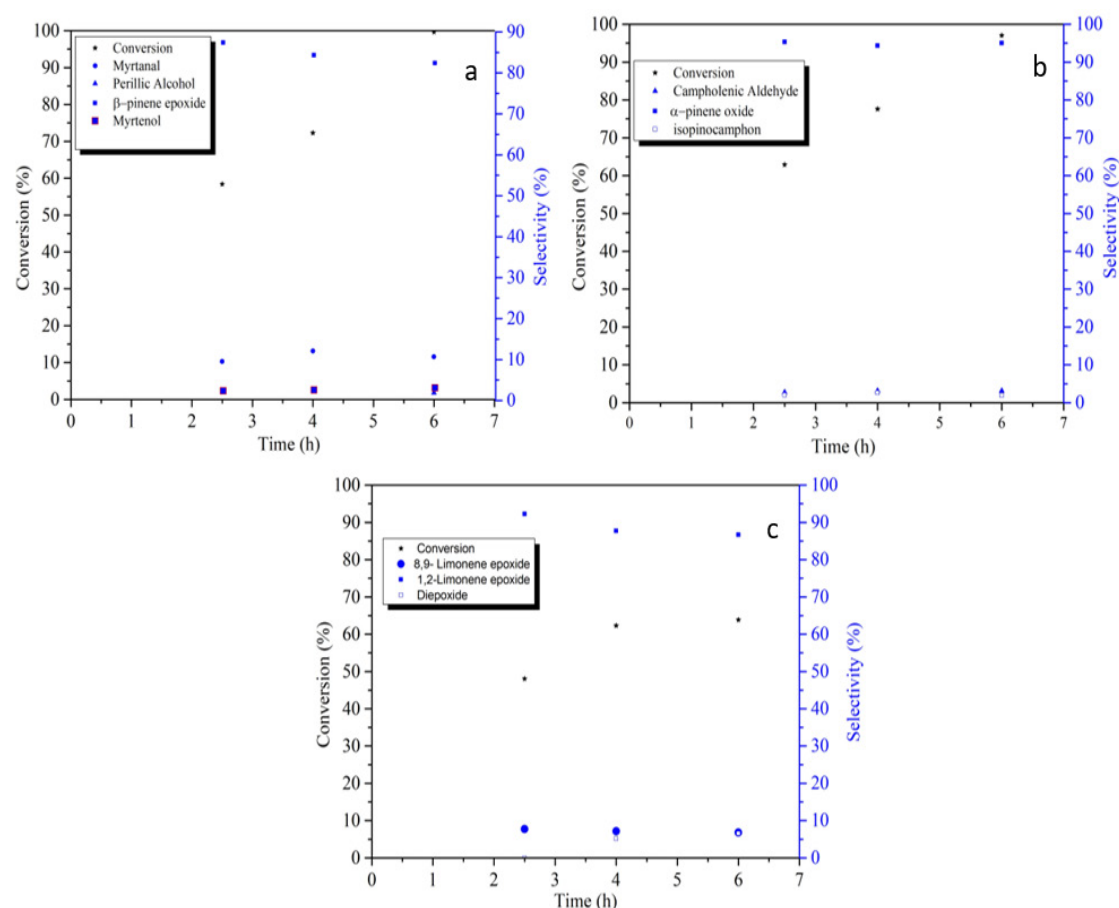


Figure 5. Conversion and selectivity in the oxidation of  $\alpha$ -pinene (a),  $\beta$ -pinene (b) and limonene (c) over ZnAC. Reaction conditions:  $50^\circ\text{C}$ , 750 rpm, 2 h, substrate :  $\text{H}_2\text{O}_2$  :  $\text{CH}_3\text{CN}$  : acetone :  $\text{H}_2\text{O}$  : catalyst mass ratio of 1 : 0.86 : 15.35 : 19.17 : 29.41 : 1.66

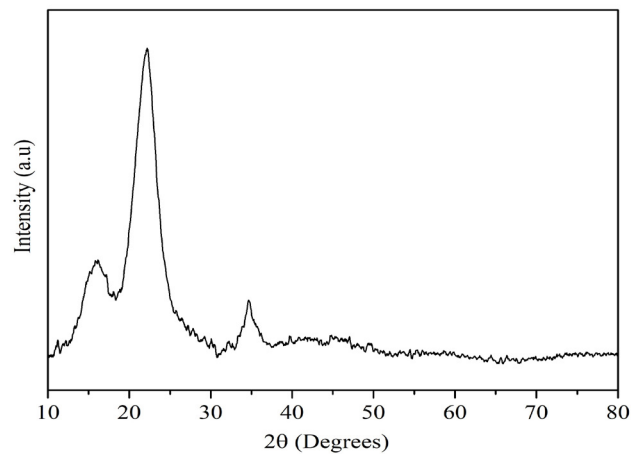


Figure. 6 X-ray spectrum of cellulose extracted from CPH

Fig. 7 presents the FTIR spectra of cellulose extracted from CPH through alkaline treatment before and after bleaching process. The FTIR spectra show characteristic bands of lignocellulosic material (lignin, cellulose, and hemicellulose). The bands at  $3505\text{ cm}^{-1}$  and  $2945\text{ cm}^{-1}$  are attributed to -OH groups and C-H stretching in methyl and methylene groups, respectively. The bands around  $1645\text{ cm}^{-1}$  correspond to the hydrogen bonding vibrations of hydroxyl groups present in cellulose (44). The bands at  $1320\text{ cm}^{-1}$ ,  $1369\text{ cm}^{-1}$ ,  $1216\text{ cm}^{-1}$ ,  $1180\text{ cm}^{-1}$ , and  $896\text{ cm}^{-1}$  correspond to C-H<sub>2</sub> deformation vibration, oscillating C-H<sub>2</sub> vibration, characteristic -COO group of hemicellulose, asymmetric C-O-C stretching vibration, and cellulose-specific oscillating C-H vibrations, respectively (44). Furthermore, it was found that there is no significant difference in the FTIR spectra after the bleaching process (images in Fig. 5); therefore, it can be inferred that this process only influences the color of cellulose and not the chemical composition of the material.

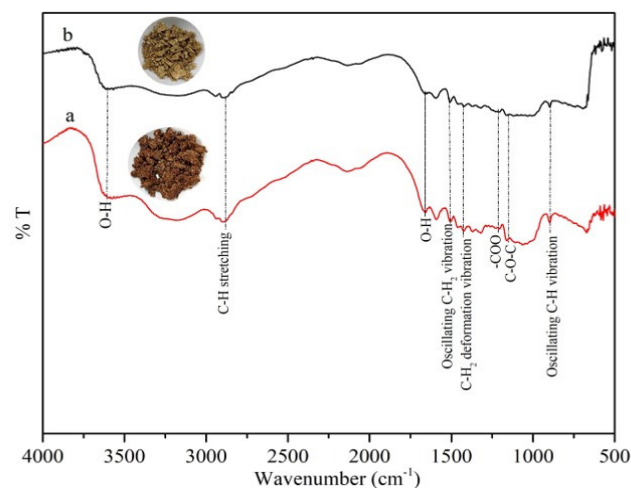


Figure 7. FTIR spectra of cellulose obtained from CPH and images of the obtained materials. Cellulose extracted from CPH by alkaline treatment (a), and cellulose extracted from CPH with alkaline treatment followed by a bleaching process (b)

The evaluation of thermal stability is important for applications that require a high processing temperature. The TGA/DTG curves of cellulose extracted from CPH are presented in Fig. 8, in which the temperature ranges in the TGA analysis for the degradation of the compounds present in the cellulose are observed. Four stages of weight loss under N<sub>2</sub> atmosphere are observed, from 20 °C to 150 °C (7.55 %), from 150 °C to 210 °C (0.51 %), from 210 °C to 380 °C (65 %), and from 380 °C to 800 °C (22.07 %). In addition, a maximum cellulose decomposition temperature of 324 °C was identified, indicating high thermal stability of the cellulose obtained, which could be used

for blending with biopolymeric materials, since it withstands the processing temperatures of poly(lactic acid) and poly(hydroxyalkanoates) (150–200 °C) used in extrusion and molding processes. This could make it a promising material for the development of rigid food packaging (trays) with reinforced structures.

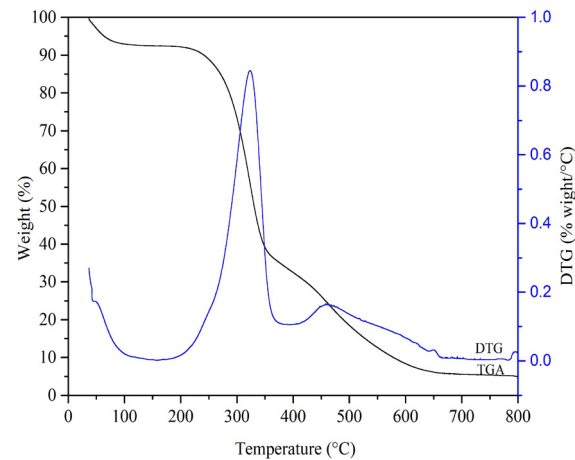
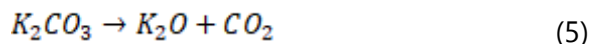


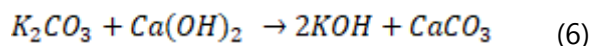
Figure 8. TGA/DTG curves of cellulose from cocoa pod husks by alkaline treatment

### Characterization of KOH

The  $K_2CO_3$  that is content in CPH is decomposed into potassium oxide ( $K_2O$ ) through a calcination process, Eq. (5). The extraction yield of  $K_2CO_3$  from CPH was 4.8% relative to the initial biomass, with a purity of 85.2%, a value that is comparable to reported purity of 86% for  $K_2CO_3$  obtained from cashew nutshell waste (45).



Furthermore, the  $K_2CO_3$  concentration is higher compared to other reported values between 12.4 and 56.7% for different agro-industrial wastes (46), and 69–81.9% for musa specie (24). Additionally, the extraction yield of KOH from causticization of  $K_2CO_3$  from CPH was 80.2%, with a concentration of 84.2%, Eq. (6), value that is comparable to reported KOH concentration (80.7%) obtained from CPH (23).



## Conclusions

Cocoa pod husks were used as a precursor to produce activated carbon, potassium hydroxide, and cellulose. The synthesized activated carbon, obtained through chemical activation with KOH, exhibited mesoporosity with a pore diameter of 10.8 nm and a specific surface area of  $468.0 \pm 1.5 \text{ m}^2/\text{g}$ ; these textural properties are suitable for using of this material in wastewater treatment and heterogeneous catalysis, a heterogeneous zinc catalyst was synthesized with promising active carbon for the epoxidation of  $\alpha$ -pinene,  $\beta$ -pinene and limonene. Cellulose was obtained through alkali treatment with a purity of 84.5%  $\alpha$ -cellulose type I, which is a promising material for biomedical application and biopolymer production; showing that CPH is an alternative for reducing the demand of cellulose from wood sources. KOH was obtained with a purity of 84.2 % from CPH extraction.

### Acknowledgements

The authors would like to express their acknowledgements to Universidad de Antioquia and the Ministry of Science, Technology, and Innovation, the Ministry of National Education, the Ministry of Industry, Trade, and Tourism, and ICETEX. Convocatoria Ecosistema Científico - Colombia Científica. Fondo Francisco José de Caldas, Contrato RC-FP44842-212-2018. Programa Bio-Reto XXI-15:50.



## CRediT authorship contribution statement

Aída Luz Villa: conceptualization, Funding acquisition, Methodology, Project administration, Supervision, Visualization, Writing – review & editing. Ana María Tovar: conceptualization, Methodology. Luis Fernando Valencia: conceptualization, Data curation, Formal analysis, Investigation, Methodology, Validation, Visualization, Writing – original draft.

## Financing

This article was financed by Universidad de Antioquia y el Ministerio de Ciencia, Tecnología e Innovación, el Ministerio de Educación Nacional, el Ministerio de Industria, Comercio y Turismo y el ICETEX. Convocatoria Ecosistema Científico – Colombia Científica. Fondo Francisco José de Caldas, Contrato RC-FP44842-212-2018. Programa Bio-Reto XXI-15:50. The authors declare that they did not receive resources for the writing or publication of this article.

## Ethical implications

The authors do not have any type of ethical involvement that should be declared in the writing and publication of this article.

## References

1. Tonini D, Albizzati PF, Astrup TF. Environmental impacts of food waste: Learnings and challenges from a case study on UK. *Waste Manag.* 2018 Mar; 76:744–766.
2. Ischia G, Fiori L. Hydrothermal Carbonization of Organic Waste and Biomass: A Review on Process. Reactor and Plant Modeling, *Waste Biomass Valor.* 2021 Oct; 12: 2797–2824.
3. Malucelli LC, Lacerda LG, Dziedzic M, da Silva MA. Preparation, properties and future perspectives of nanocrystals from agro-industrial residues: a review of recent research, *Rev. Environ. Sci. and Biotechnology.* 2017 Feb; 16(1): 131–145.
4. Prado I, Cubrero J, Lu TA, Eibes G. Integral multi-valorization of agro-industrial wastes: A review. *Waste Management.* 2024 Jun; 183:42–52.
5. Abbott PC, Benjamin TJ, Burniske GR, Croft MM, Fenton MC, Lundy RF et al. An Analysis of the Supply Chain of Cacao in Colombia, United States Agency for International Development - USAID. 2018 Oct.
6. Bello O., Sian, TT, Ahmad MA. Adsorption of Remazol Brilliant Violet-5R reactive dye from aqueous solution by cocoa pod husk-based activated carbon: Kinetic, equilibrium and thermodynamic studies, *Asia-Pac. J. Chem. Eng.* 2012 Mar; 7(3): 378–388.
7. Meza-Sepúlveda DC, Castro AM, Zamora A, Arboleda JW, Gallego AM, Camargo-Rodríguez AV. Bio-based value chains potential in the management of cacao pod waste in Colombia, a case study, *Agronomy.* 2021 Abr; 11(4): 693.
8. Lu F, Rodriguez J, Van DI, Westwood NJ, Shaw L, Robinson JS et al. Valorisation strategies for cocoa pod husk and its fractions, *Curr. Opin. Green Sustain. Chem.* 2018 Jul; 14: 80–88.
9. Belwal T, Cravotto C, Ramola S, Thakur M, Chemat F, Cravotto G. Bioactive Compounds from Cocoa Husk: Extraction, Analysis and Applications in Food Production Chain, *Foods.* 2022 Mar; 11: 798.
10. Tea K, Igor K, Kiril D. Cocoa husk biomass conversion for application in fibre packaging, *Biomass Convers. Biorefin.* 2022 Oct.
11. Tingaut P, Zimmermann T, Sèbe G. Cellulose nanocrystals and microfibrillated cellulose as building blocks for the design of hierarchical functional materials, *J. Mater. Chem.* 2012 Jul; 22(38) 20105–20111
12. Luo L, Lan Y, Zhang Q, Deng J, Luo L, Zeng Q et al. A review on biomass-derived activated carbon as electrode materials for energy storage supercapacitors. *Journal of Energy Storage.* 2022 Nov; 55.





13. Yahya MA, Al-Qodah Z, Ngah WZ. Agricultural bio-waste materials as potential sustainable precursors used for activated carbon production: A review, *Renew. Sust. Energ. Rev.* 2015 Jun; 46:218–235.
14. Bonvehí JS, Coll FV. Protein quality assessment in cocoa husk. *Food Res. Int.* 1999 Abr; 32: 201–208.
15. Babayemi JO, Adewuyi GO, Dauda KT, Kayode AA. The Ancient Alkali Production Technology and the Modern Improvement. *Asian J. Appl. Sci.* 2011; 4: 22–29.
16. Arueya GL, Sharon OO. Characterization of Dutch-Cocoa produced using potash extract from cocoa pod husk as an alkalizing bioresource, *Braz. J. Food Technol., Campinas.* 2023; 26: 1 - 15.
17. Daniyan IA, Mpofu K, Daniyan OL, Adeodu AO, Uchegbu ID. Design and Modelling of Automated Reactor for the Production of Caustic Potash from Cocoa Pod Husk. *Procedia CIRP.* 2019; 84 :960–965.
18. Tsai WT, Bai YC, Lin YQ, Lai YC, Tsai CH. Porous and adsorption properties of activated carbon prepared from cocoa pod husk by chemical activation, *Biomass Convers Biorefin.* 2020 Mar ;10(1): 35–43.
19. Dos Santos DM, Bukzem A, Ascheri PR, Signini R, De Aquino LB. Microwave-assisted carboxymethylation of cellulose extracted from brewer's spent grain. *Carbohydr. Polym.* 2015 Jun; 131: 125–133.
20. Ogundiran MB, Babayemi JO, Nzeribe CG. Determination of metal content and an assessment of the potential use of waste cashew nut ash (CNSA) as a source for potash production, *Bioresources.* 2011; 6(1):529 – 536.
21. García M, Soto H, Peralta E, Carvajal E, Madera T, Lomelí M et al. Production and Characterization of Cellulosic Pulp from Mango Agro-Industrial Waste and Potential Applications, *Polymers.* 2023 Jul; 15: 3163.
22. Ofori P. Production of potassium hydroxide (KOH) from plant biomass: the case of cocoa pod husks and plantain peels. [tesis doctoral en internet]. Kumasi – Ghana; 2017 [citada 16 Ene 2024]. 66 p. Disponible en :<https://www.researchgate.net/publication/340298729> (2017).
23. Babayemi JO, Dauda KT, Kayode AA, Nwude DO, Ajiboye JA, Essien ER et al. Determination of potash alkali and metal contents of ashes obtained from peels of some varieties of nigeria grown musa species, *Bioresources.* 2010; 5(3): 1384 – 1392.
24. Londoño-Larrea P, Villamarin-Barriga E, García AN, Marcilla A. Study of Cocoa Pod Husks Thermal Decomposition. *Appl. Sci.* 2022 Sep; 12(18) 9318
25. Díez D, Urueña A, Piñero R, Barrio A, Tamminen T. Determination of hemicellulose, cellulose, and lignin content in different types of biomasses by thermogravimetric analysis and pseudocomponent kinetic model (TGA-PKM Method), *Processes.* 2020 Ago; 8(9): 1048.
26. Eletta OA, Adeniyi AG, Ighalo JO, Onifade DV, Ayandele FO. Valorisation of Cocoa (*Theobroma cacao*) pod husk as precursors for the production of adsorbents for water treatment, *Environ. Technol. Rev.* 2020 Feb; 9(1):20–36.
27. Villota SM, Lei H, Villota E, Qian M, Lavarias J, Taylan V et al. Microwave-Assisted Activation of Waste Cocoa Pod Husk by  $H_3PO_4$  and KOH - Comparative Insight into Textural Properties and Pore Development, *ACS Omega.* 2019 Abr; 4(4):7088–7095.
28. Ateş F, Özcan Ö. Preparation and Characterization of Activated Carbon from Poplar Sawdust by Chemical Activation: Comparison of Different Activating Agents and Carbonization Temperature, *Eur. J., Eng. Sci., Tech.* 2018 Nov; 3(11): 6–11.
29. Chen R, Lia L, Liua Z, Luc M, Wanga C, Lia H, Maa W, Wang S. Preparation and characterization of activated carbons from tobacco stem by chemical activation, *J. Air Waste Manage Assoc.* 2017 Abr; 67(6): 713–724.

30. Muniandy L, Adam F, Mohamed AR, Ng EP. The synthesis and characterization of high purity mixed microporous/mesoporous activated carbon from rice husk using chemical activation with NaOH and KOH, *Microporous Mesoporous Mater.* 2014 Jun; 197: 316–323.
31. Prakash MO, Raghavendra G, Ojha S, Panchal M. Characterization of porous activated carbon prepared from arhar stalks by single step chemical activation method, in *Materials Today: Proceedings.* 2020 Jun; 39(4) 1476–148.
32. Lessa OA, Tavares IM, Souza LO, Pimenta LG, Cordazzo M, Tonoli HD et al. New biodegradable film produced from cocoa shell nanofibrils containing bioactive compounds. *J. Coat. Technol. Res.* 2021 Sep; 18(6):1613–1624.
33. Gomez E, Nunell G, Cukierman AL, Bonelli P. Agroindustrial waste conversion into ultramicroporous activated carbons for greenhouse gases adsorption-based processes, *Bioresour. Technol. Rep.* 2022 Jun; 18:101008.
34. Oginni O, Singh K, Oporto G, Dawson B, McDonald L, Sabolsky E. Influence of one-step and two-step KOH activation on activated carbon characteristics, *Bioresour. Technol. Rep.* 2019 Jun; 7.
35. García D, Jaramillo M, Bustamante F, Villa L, Alarcon E. Epoxidation of  $\beta$ -pinene with a highly-active and low-cost catalyst, *Braz. J. Chem. Eng.* 2020 Nov; 38: 89-100.
36. Prado KS, Spinacé AS. Isolation and characterization of cellulose nanocrystals from pineapple crown waste and their potential uses, *Int. J. Biol. Macromol.* 2018 Oct; 122: 410–416.
37. Hafemann E, Battisti R, Marangoni C, Machado AF. Valorization of royal palm tree agroindustrial waste by isolating cellulose nanocrystals, *Carbohydr. Polym.* 2019 May; 218:188–198.
38. Henrique MA, Silvério HA, Neto PF, Pasquini D. Valorization of an agro-industrial waste, mango seed, by the extraction and characterization of its cellulose nanocrystals, *J. Environ. Manage.* 2013 Feb; 121: 202–209.
39. Nang v, Chi H, Duy T, Thanh T, Van P, Van L. Extraction of High Crystalline Nanocellulose from Biorenewable Sources of Vietnamese Agricultural Wastes, *J Polym Environ.* 2020 Mar; 28:1465-1474.
40. Nada MA, El-Kady MY, El-sayed ES, Amine FM. Preparation and characterization of microcrystalline cellulose (MCC). *Bioresources.* 2009 Sep; 4(4): 1359-1371.
41. Jiang J, Zhu Y, Jiang F. Sustainable isolation of nanocellulose from cellulose and lignocellulosic feedstocks: Recent progress and perspectives. *Carbohydrate polymers.* 2021 Sep; 267, 1–21.
42. Mekuye B, Abera B. Nanomaterials: An overview of synthesis, classification, characterization, and applications. *Nano Select.* 2023 Jun; 4:486-501.
43. Tyshkunova IV, Poshina, DN, Skorik, Y. Cellulose Cryogels as Promising Materials for Biomedical Applications. *Int. J. Mol. Sci.* 2022 Feb; 23 (4): 2037.
44. Mazlita Y, Lee HV, Hamid BA. Preparation of cellulose nanocrystals bio-polymer from agro-industrial wastes: Separation and characterization, *Polym. Polym. Compos.* 2016; 24(9): 719–728.
45. Taiwo AA, Oluwadare I, Shobo AO, Amolegbe SA. Extraction and potential application of caustic potash from kolanut husk, uguwu pod husk and plantain peels, *Scientific Research and Essay.* 2008 Oct; 3 (10):515-517.
46. Taiwo OE, Osinowo AO. Evaluation of various agro-wastes for traditional black soap production. *Bioresour. Technol.* 2001 Ago; 79(1): 95–97.